

Lasers in Manufacturing Conference 2023

Laser-based crystallization of oxide ceramic thin films for solid oxide fuel cells

Jonas Frühling^{a,*}, Sarah Schreyer^a, Samuel Fink^a, Christian Vedder^a

^aFraunhofer Institute for Laser Technology (ILT), Steinbachstraße 15, 52074 Aachen, Germany

Abstract

Solid Oxide Fuel Cells show the highest efficiency of all available fuel cell types. However, this technology is still subject to limitations, such as insufficient cycling stability and long start-up times. With the use of a thin proton-conducting electrolyte and a metallic support it is expected to overcome these limitations.

To manufacture such a cell, the membrane electrode assembly is wet-chemically deposited onto the metallic support and then thermally crystallized. Conventional methods (Rapid Thermal Annealing or oven) lead to unwanted interactions with the substrate material. The use of a laser beam for thermal crystallization of the thin films allows very short processing times and therefore offers the potential to completely crystallize the thin films without the formation of minor phases. In this work electrolyte material is crystallized using a laser beam, and the influence of different process parameters is investigated using X-ray diffraction and transmission electron microscopy.

Keywords: solid oxide fuel cells; laser processing; crystallization; thin films

1. Motivation

In the course of the energy transition, interest in various P2P (power-to-power) technologies has increased in recent years. These are needed to balance power peaks and troughs from fluctuating renewable energy sources such as solar or wind power. A suitable technology for this is the chemical storage of the generated electricity in hydrogen and the subsequent conversion back into electricity. Crucial to the successful implementation of a hydrogen-based P2P pathway is the overall efficiency of the conversion chain, which can be described by the PFP (Power-2-Fuel-2-Power index) (Grinberg et al., 2016). The high-temperature fuel cell and electrolyzer cell (SOFC: Solid Oxide Fuel Cell; SOEC: Solid Oxide Electrolyzer Cell) based on oxide ceramic materials have the higher PFP compared to low-temperature cells such as PEMFC (Proton Exchange Membrane Fuel Cell) and PEMEC (Proton Exchange Membrane Electrolyzer Cell (Hayashi et al., 2009). However, this technology is still subject to limitations today, such as insufficient tolerance to thermal/redox cycling, a long start-up time and high operating temperatures. Metal supported fuel cells with a proton conducting thin film

electrolyte are a promising alternative to the state-of-the-art anode supported cells with an oxide ion conducting electrolyte.

The deposition of the individual functional layers (anode, electrolyte, cathode) on the metallic substrate can be done by vacuum processes (especially PLD: Pulsed Laser Deposition) or wet chemical processes. In both cases, a thermal post-treatment of the deposited layers is required to achieve the desired crystallinity. By using laser radiation for thermal post-treatment, the holding time of the temperatures required for this can be reduced by several orders of magnitude. This potentially reduces unwanted reactions of the functional materials with the metallic substrate material, such as oxidation or diffusion.

In this work, the laser-based crystallization of the proton conducting electrolyte material BZY (Yttrium-doped Barium Zirconate) on a metallic substrate is investigated.

2. Sample preparation and experimental setup

A BZY precursor solution with an yttrium content of 10 at% was used as starting material. Alloy C276 sheets with dimensions of 25 mm x 25 mm x 2 mm were used as substrates. The solution was deposited onto the substrate using a spin coater. After deposition, the films were pyrolyzed at 400 °C for 5 minutes on a hot plate to remove the remaining organic components. Samples with two coatings were used. Therefore, the coating process was repeated a second time after pyrolysis.

The experimental setup for the laser process is shown in Fig. 1 (a). The main components are the laser source and a coaxial integrated pyrometer including a controller. The sample is placed in a sample holder on a two-axes handling system and is moved under the laser beam in unidirectional paths. The laser source is a diode laser of the type Compact Evolution DILAS Diodenlaser GmbH with a maximum output power of 450 W (continuous wave, $\lambda = 980$ nm). The laser beam has a quadratic top-hat profile with 600 μm edge length in the focal plane (Fig. 1 (b)). During the process the heat radiation is detected by the pyrometer. The measuring spot of the pyrometer has a diameter of about 450 μm . The pyrometer is used to adjust the laser power to maintain a set temperature T_{set} . Due to an inhomogeneous temperature field in the measuring spot, the set temperature is not the true temperature.

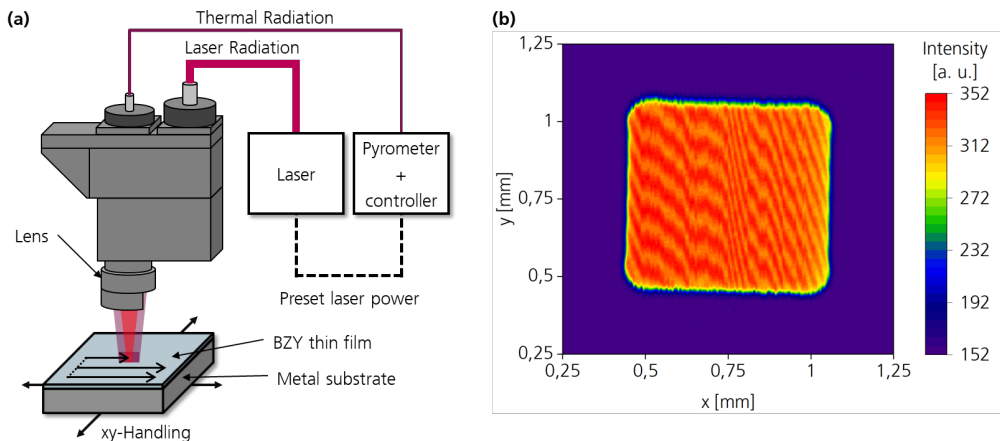


Fig. 1. (a) Experimental setup; (b) Laser intensity distribution

Different set temperatures ($T_{\text{set}} = 700\text{ °C} - 900\text{ °C}$) and different interaction times ($t = 10\text{ ms} - 1000\text{ ms}$) were investigated. The interaction time corresponds to the time a position is exposed to the laser beam and results from the quotient of spot diameter and feed rate. The spacing between the lines is $600\text{ }\mu\text{m}$.

3. Results

First, a parameter study was carried out to investigate the influence of the main process parameters, namely set temperature T_{set} and interaction time t on the resulting crystallographic structure. These were investigated with a XRD of the type Bruker Advance D8 having a Cu X-ray tube ($\lambda = 1.45059\text{ \AA}$). The measurement was carried out in Bragg-Brentano geometry in a 2-Theta range of 20° to 80° .

To quantify the phase fraction of the target phase BZY and the unwanted minor phase BaMoO_4 , the integral over the peaks assigned to each phase was determined. BaMoO_4 contains elements from both the substrate material (Mo) and the layer material (Ba). This suggests diffusion of Mo into the BZY thin film and subsequent disintegration of the perovskite structure of BZY. The integrated peak intensities of BZY and BaMoO_4 are shown in Fig 2 as a function of interaction time for different set temperatures.

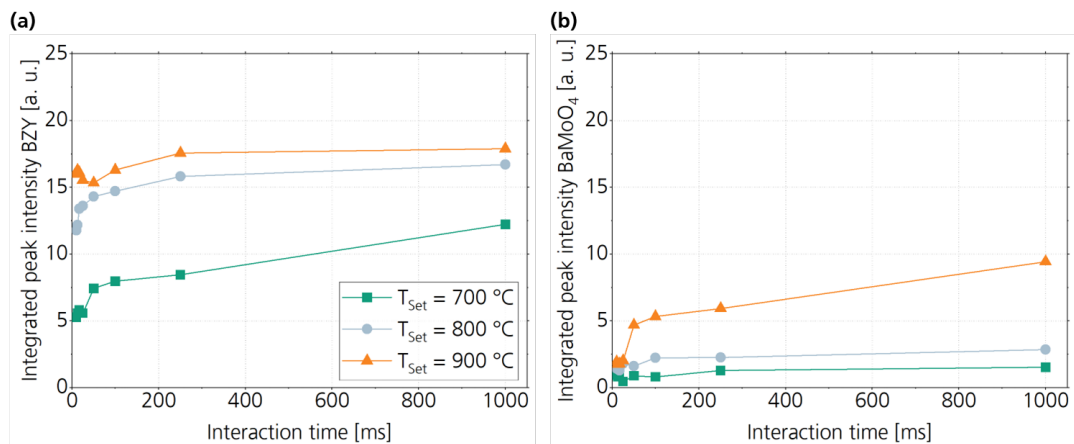


Fig. 2. Integrated peak intensities of BZY (a) and BaMoO_4 (b) for different set temperatures as a function of interaction time.

An increase of interaction time and set temperature lead to an increase of integrated peak intensity of BZY and BaMoO_4 . The integrated peak intensity of BZY shows an asymptotic trend. This indicates an almost complete crystallization for sufficiently large interaction times and set temperatures. For set temperatures of 800 °C and 900 °C a process range can be determined in which nearly complete crystallization of the BZY is achieved while avoiding the formation of BaMoO_4 . For a set temperature of $T_{\text{set}} = 800\text{ °C}$ this is the case for interaction times $t \geq 100\text{ ms}$ and for $T_{\text{set}} = 900\text{ °C}$ for $t \leq 25\text{ ms}$ in the investigated process window.

In addition to crystallinity, the crystallite size was also investigated using XRD measurements. Since the proton conductivity of BZY is limited by the grain boundaries large crystallites are desirable. The crystallite size was calculated using the commercial software DIFFRAC.TOPAS from Bruker AXS GmbH. This was possible only for samples with sufficiently large integrated peak intensity of BZY and sufficiently small of BaMoO_4 . The calculated crystallite sizes are shown in Fig. 3.

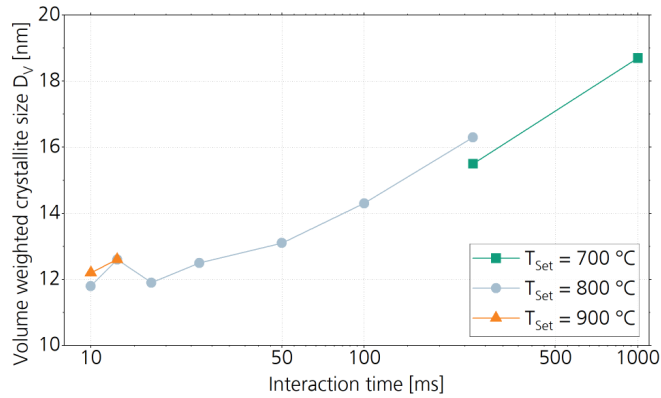


Fig. 3. Volume weighted crystallite size of BZY for different set temperatures as a function of interaction time.

An increase of interaction time leads to an increase in crystallite size. The set temperature has no significant influence on the crystallite size in the investigated parameter range. The calculated crystallite size is between 11 nm and 19 nm for all investigated parameters.

To validate the calculated crystallite sizes, TEM images of a thin film crystallized by laser radiation ($T_{\text{Set}} = 800\text{ °C}$, $t = 16.7\text{ ms}$) and a reference sample were taken. For the reference sample, a platinized silicon wafer was coated with BZY and then annealed in an RTA (Rapid Thermal Annealing) for 800 °C and 10 minutes. The TEM images of both samples are shown in Fig. 4.

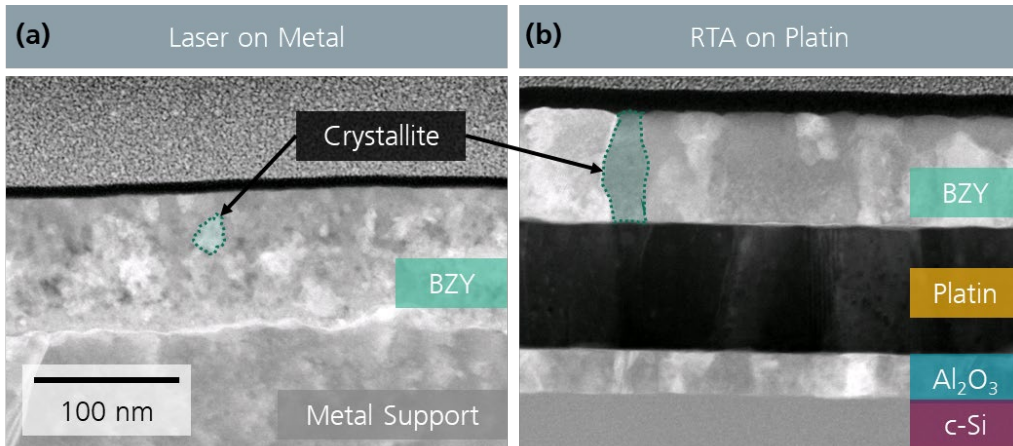


Fig. 4. TEM images of BZY thin film on a C276 support processed by laser radiation (a) and of a BZY thin film on a platinized silicon wafer crystallized by RTA

The TEM image of the laser annealed sample shows a non-uniform crystallite size of the BZY layer. The observed crystallite sizes range from 5 nm to 26 nm. The crystallite size of 12.3 nm determined by DIFFRAC.TOPAS is compatible. In comparison, the crystallites of the thin film annealed by RTA on platinum are significantly larger and of the same order of magnitude as its layer thickness. A possible reason for this, besides the longer temperature hold time, may be the lattice constant of platinum, which at 4.0 Å is much more similar to that of BZY (4.2 Å) than that of the metallic C276 substrate (3.6 Å). A similar lattice constant can lead to an improved crystal growth (Kim et al., 2011).

4. Conclusion and outlook

The results of a parameter study for laser-based crystallization of BZY thin films on metallic substrates are presented. Single-phase crystallization of the BZY perovskite structure without unwanted minor phases such as BaMoO₄ is possible. The formation of minor phases can be avoided if short interaction times are used. Furthermore, the crystallite sizes of the laser annealed thin films were investigated using XRD and TEM. The crystallite sizes observed by TEM range from 5 nm to 26 nm and are still smaller than the crystallite sizes of RTA annealed thin films. Next steps are the investigation of approaches to increase the crystallite size of BZY thin films and the crystallization of a complete membrane electrode assembly.

Acknowledgements

The presented research was partly funded by the German Federal Ministry of Economic Affairs and Climate Action within the framework "IGF". The authors would like to thank the consortium for the excellent cooperation within the project "NextSOFC" (IGF 21965 N). The authors are responsible for the content.

References

- Grinberg Dana, A., Elishav, O., Bardow, A., Shter, G., & Grader, G. (2016). Nitrogen-Based Fuels: A Power-to-Fuel-to-Power Analysis. *Angewandte Chemie (International Ed.)*, 55(31), 8798-8805.
- Hayashi, Katsuya; Yokoo, Masayuki; Yoshida, Yoshiteru; Arai, Hajime (2009): Solid Oxide Fuel Cell Stack with High Electrical Efficiency. In: *NTT Group R&D for Reducing Environmental Load (Vol. 7)*.
- KIM, Young Beom ; GÜR, Turgut M. ; JUNG, Hee-Joon ; KANG, Sangkyun ; SINCLAIR, Robert ; PRINZ, Fritz B.: Effect of crystallinity on proton conductivity in yttrium-doped barium zirconate thin films. In: *Solid State Ionics* 2011, Nr. 198, S. 39–46